Medicine®

QUALITY IMPROVEMENT STUDY

OPEN

# SEMAC-VAT MR Imaging Unravels Peri-instrumentation Lesions in Patients With Attendant Symptoms After Spinal Surgery

*Shun Qi, Zhi-Gang Wu, Yun-Feng Mu, Lang-Lang Gao, Jian Yang, Pan-Li Zuo, Mathias Nittka, Ying Liu, Hai-Qiang Wang, and Hong Yin*

**Abstract:** The study aimed for evaluating the diagnostic value of a 2D Turbo Spin Echo (TSE) magnetic resonance (MR) imaging sequence implanted slice-encoding metal artifact correction (SEMAC) and view-angle tilting (VAT) in patients with spinal instrumentation.

Sixty-seven consecutive patients with an average age of 59.7 ± 17.8 years old (range: 32–75 years) were enrolled in this study. Both sagittal, axial T1-weighted and T2-weighted MRI images were acquired with a standard TSE sequence and a high-bandwidth TSE sequence implemented the SEMAC and VAT techniques. Three continuous sections around the instrumentation in axial and sagittal images were selected for quantitative evaluation. The measurement included cumulative areas of signal void on axial images and the length of spinal canal obscuration on sagittal images. Three radiologists independently evaluated all images blindly. The inter-observer reliability was evaluated with inter-class coefficient. We defined patients with discomfortable symptoms caused by spinal instrumentation as spinal instrumentation adverse reaction.

Visualizations of all periprosthetic anatomic structures were significantly better for SEMAC-VAT compared with standard imaging. For axial images, the area of signal void at the level of the instrumentation were statistically reduced with SEMAC-VAT TSE sequences than with standard TSE sequences for T2-weighted images ($9.9 \pm 2.6\,cm^2$ vs $29.8 \pm 14.7\,cm^2$, $P < 0.001$). For sagittal imaging, the length of spinal canal obscuration at the level of the instrumentation was reduced from $5.2 \pm 2.0$ cm to $1.2 \pm 0.6$ cm on T2-weighted images ($P < 0.001$), and from $4.8 \pm 2.1$ cm to $1.1 \pm 0.5$ cm on T1-weighted images with SEMAC-VAT sequences ($P < 0.001$). Interobserver agreement for visualization of anatomic structures and image quality was good for both SEMAC-VAT (k = 0.77 and 0.68, respectively) and standard (k = 0.74 and 0.80, respectively) imaging. The number of abnormal findings noted on SEMAC images (59 findings) was significantly higher than detected on standard images (40 findings). The incidence rate of spinal instrumentation adverse reaction was 38.81%.

MR images with SEMAC-VAT can significantly reduce metal artifacts for spinal instrumentation and improve delineation of the instrumentation and periprosthetic region. Furthermore, SEMAC-VAT technique can improve diagnostic accuracy in patients with post-instrumentation spinal diseases.

(*Medicine* 95(14):e3184)

**Abbreviations**: MR = magnetic resonance, SEMAC = slice-encoding metal artifact correction, VAT = view-angle tilting.

## INTRODUCTION

Metallic spinal implants are commonly used in patients with spinal disorders. Despite spinal instrumentation can increase fusion rate of spinal surgery, a variety of adverse postoperative effects have been noted and well documented in the literature. The adverse effects include metal hypersensitivity, edema, infection, and spinal cord compression occurring early after surgery, as well as tumor recurrence, implant loosening, and osteolysis in long-term run. Severe adverse effects affecting the life quality of patients might inevitably need revision, which consequently impose heavy load on patients in terms of health and economic issues.

Magnetic resonance (MR) imaging has become an important modality for spinal imaging due to its superiority in the assessment of the spinal cord, adjacent soft tissues, and osseous structures. For postoperative patients with spinal instrumentation, current MRI is limited in the evaluation of periprosthetic complications due to magnetic susceptibility artifacts and eddy current artifacts induced by metallic implants.[1–4] There are 2 types of distortions. Through-plane distortions are derived from a distorted excitation profile during slice-selective excitation, and in-plane distortions are derived from disrupted frequency encoding during the process of readout. Therefore, various MR techniques are being developed to reduce metallic artifacts. It has been reported that view angle tilting (VAT) Turbo Spin Echo (TSE) sequence combined with high radio frequency and

Editor: Giancarlo Carli.
Received: August 5, 2015; revised: March 1, 2016; accepted: March 3, 2016.
From the Department of Radiology (SQ, LLG, YL, HY), Xijing Hospital, the Fourth Military Medical University, Xi'an, PR China; Department of Orthopaedics (ZGW), No. 518 Hospital of Chinese People's Liberation Army, Xi'an, PR China; Department of Orthopedics (ZGW), Lanzhou General Hospital of Lanzhou Military Region, People's Liberation Army, Lanzhou, PR China; Department of Radiotherapy (YFM), Xijing Hospital, the Fourth Military Medical University, Xi'an, PR China; Department of Radiology (SQ, JY), The First Affiliated Hospital of Medical College of Xi'an Jiaotong University, Xi'an, PR China; Siemens Healthcare (PLZ), MR Collaborations NE Asia, Beijing, PR China; Siemens Healthcare (MN), Erlangen, Germany; and Department of Orthopaedics (HQW), Xijing Hospital, The Fourth Military Medical University, Xi'an, PR China.

Correspondence: Ying Liu, Department of Radiology, Hai-Qing Wang, Department of Orthopaedics, and Hong Yin, Department of Radiology, Xijing Hospital, the Fourth Military Medical University, No. 15 Changlexi Road, Xi'an 710032, PR China (e-mail: yingyinglyly@126.com, hqwang@fmmu.edu.cn, yinhong@fmmu.edu.cn).

YL, HQW, and HY conceived and designed the experiment. SQ and ZGW performed the experiments. YFM and LLG contributed the acquisition of data. JY, PLZ and MN analyzed and interpreted the data. SQ, ZGW and MN wrote the article. All authors contributed to the study in significant ways and have approved the final article.

SQ and ZGW contributed equally to this work.

This research was supported by China Postdoctoral Science Foundation (Grant no.: 2015M572803) and Academic Pushing Project of Xijing Hospital (Grant no.:XJZT14M06).

The authors have no conflicts of interest to disclose.



ISSN: 0025-7974
DOI: 10.1097/MD.0000000000003184

readout bandwidths successfully suppresses in-plane distortions rather than through-plane distortions.[5–8] By extending the VAT TSE sequence with additional phase-encoding along slice-selective z-axis, slice-encoding metal artifact correction (SEMAC) corrects the through-plane distortions using the additional z-phase encoding to restore the distorted signal to their actual slice location.[5,9,10]

Several studies have demonstrated the efficacy of SEMAC-VAT technique in eliminating metal artifacts in animal models and in patients with metal implants in the spine, hips, knees, and the brain.[11–16] However, few studies systematically addressed the diagnostic value of SEMAC-VAT technique for clinical use, in particular for patients with clinically diagnosed discomfortable symptoms. Nevertheless, it is generally believed that instrumentation with titanium alloy is the most compatible type of metal, rarely causing adverse effects.

This study aimed for evaluating the diagnostic value of SEMAC-VAT sequence in patients with titanium pedicle screws as spinal instrumentation who had been reported having discomfortable symptoms.

## METHODS

### Patients and Study Design

This study was approved by the Institutional Ethics Review Board with written informed consent obtained from all patients. Consecutive patients undergoing spinal instrumentation surgery, who were recommended to perform MRI scan from June 2014 to May 2015, were included in this study. The enrolling criteria included patients who complained discomfort after spinal surgery using titanium alloy pedicle screws. We defined patients with discomfortable symptoms caused by spinal instrumentation as spinal instrumentation adverse reaction.

### MR Imaging

All patients were examined on a 1.5 T MR scanner (MAGNETOM Aera, Siemens AG, Erlangen, Germany) using the integrated spine coil. The T1-weighted sagittal, T2-weighted sagittal, and axial images were acquired using a standard TSE sequence and prototype TSE sequence implementing the SEMAC-VAT technique. The imaging parameters are summarized in Table 1.

### Quantitative Image Analysis

A musculoskeletal radiologist (with 6 years of experience) measured the cumulative area of signal void on the T2-weighted axial image, which was defined as the area without discernible anatomic information, including both low- and high-signal-intensity artifacts induced by the instrumentation (Figure 1A). Length of spinal canal obscuration on the T1- and T2-weighted sagittal image between the 2 sequences was also evaluated (Figure 1B). Three continuous sections at the level of the instrumentation in axial and sagittal images were selected for the evaluation. The reader compared the following 2 sets of the same level of axial/sagittal MR images in random order.

### Qualitative Image Analysis

Three musculoskeletal radiologists (with 6 and 7 years of experience) independently compared the standard TSE images with the SEMAC-VAT TSE images. Visibility of 4 periprosthetic anatomic structures including visualization of the pedicle (near the screw), vertebral body (near the screw), dural sac (between the affected intervertebral disc level), and intervertebral neural foramina (near the screw) in the paired MR images were graded as follows: grade 1, the periprosthetic region is barely delineated; grade 2, <25% of the structures; grade 3, 25% to 50% of the structures; grade 4, 50% to 75% of the structures; and grade 5, >75% of the structures.[17]

Image quality including geometric image distortion, spatial blurring, and image noise was assessed on the following criteria: score of 1, severe artifacts and nondiagnostic image; 2, moderate artifacts with moderate impairment of diagnostic quality; 3, visible artifacts without impairment of diagnostic quality; 4, barely visible artifacts; and 5, no artifacts.[18] If abnormal imaging findings were present, such as osteolysis, loosening, edema, and infection, this was recorded and the number of such findings per sequence was noted.

All of the images were evaluated in a random order. The readers were blinded to the scores of the corresponding previous images. To minimize the learning bias, patients' information and the imaging parameters were hidden.

### Statistical Analysis

All analyses were performed with statistical software SPSS (version 17.0, SPSS Inc, Chicago, IL). Differences in signal void size and length of spinal canal obscuration were assessed by using the paired *t* test, and differences in qualitative data (visualizations of anatomic structures and image quality) were assessed with the Wilcoxon signed-rank test. Data were shown as mean ± standard deviations, with $P < 0.05$ as a statistically significant difference. The number of discordant cases of

**TABLE 1.** MRI Parameters

| | T1-Weighted Sagittal | | T2-Weighted Sagittal | | T2-Weighted Axial | |
|---|---|---|---|---|---|---|
| | **Standard** | **SEMAC-VAT** | **Standard** | **SEMAC-VAT** | **Standard** | **SEMAC-VAT** |
| TE/TR (ms) | 7/608 | 7/682 | 74/3380 | 79/3300 | 82/3000 | 81/3490 |
| ETL | 3 | 7 | 17 | 23 | 17 | 23 |
| FOV ($cm^2$) | 320 × 320 | 320 × 320 | 200 × 200 | | | |
| Matrix | 320 × 256 | 320 × 224 | 320 × 224 | | | |
| Thickness (cm) | 3 | 3 | 4 | | | |
| TA (min) | 1:27 | 4:25 | 1:12 | 2:43 | 2:06 | 2:53 |
| Readout bandwidth (Hz/pixel) | 235 | 600 | 200 | 540 | 190 | 540 |
| z-phase encoding steps | 0 | 6 | 0 | 6 | 0 | 6 |

SEMAC-VAT = slice-encoding metal artifact correction–view-angle tilting.

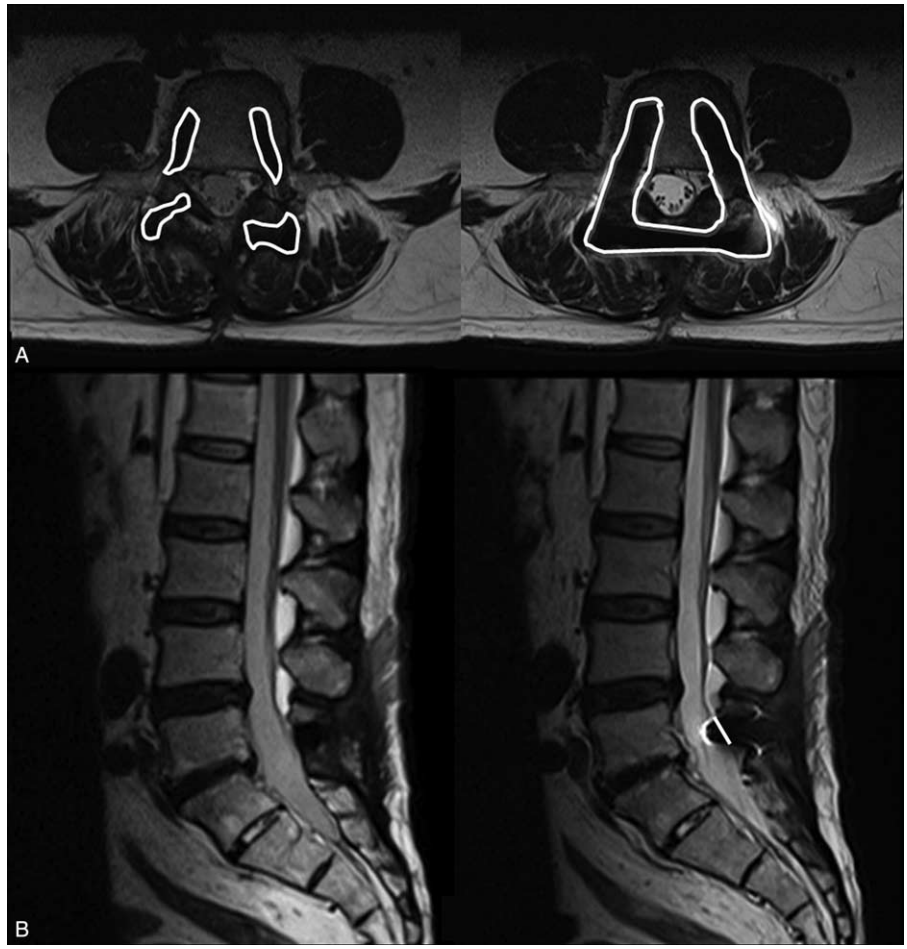


**FIGURE 1.** Quantitative evaluation of standard TSE and SEMAC-VAT sequences in spinal imaging. Signal void area in the axial images was measured as the area without discernible anatomic information in the solid line circles (A), and the length of spinal canal obscuration in the sagittal images was measured as the length of the solid line (B). SEMAC-VAT = slice-encoding metal artifact correction–view-angle tilting, TSE = Turbo Spin Echo.

abnormal imaging findings detected by the 2 different MR sequences were analyzed with a McNemar test. Interobserver agreement between the 2 readers was determined by Kappa analysis. A k value of 0 indicated poor agreement; 0.01 to 0.20, slight agreement; 0.21 to 0.40, fair agreement; 0.41 to 0.60, moderate agreement; 0.61 to 0.80, good agreement; and 0.81 to 1.00, excellent agreement.

## RESULTS

### Patients

One hundred and forty-two patients with spinal instrumentation who were recommended to perform spinal MR scan were enrolled in this study prospectively. Among them, 44 patients were excluded for no discomfortable symptoms related to the spinal instrumentation, 5 patients were excluded for incomplete scan caused by claustrophobia, 15 patients were excluded for incomplete scan caused by pain or discomfort, and 11 patients were excluded for images with motion artifacts. Finally, images from 67 consecutive patients (M:F = 41:26; age range, 32–75 years; mean age, $59.7 \pm 17.8$ years) were analyzed in the study (Figure 2). There were 24 patients for cervical spinal MRI, 9 patients for thoracic spinal MRI, and 34 patients for lumbar spinal MRI. The average spinal segments for fixation were 2.97 levels: 2 segments for 23 patients, 3 segments for 29 patients, 4 segments for 10 patients, 5 segments for 4 patients, and 6 segments for 1 patient. The primary diseases included disc herniation (n = 35), spinal primary tumors (n = 15), spinal metastasis (n = 7), spinal tuberculosis (n = 9), and spinal fractures (n = 12). And the reasons of postoperative MR imaging were lumbar pain (n = 29), cervical pain (n = 22), back pain (n = 6), and fever (n = 10).

### Quantitative and Qualitative Results

On T2-weighted axial images, the area of signal void around the instrumentation was significantly reduced when using SEMAC-VAT sequences ($9.9 \pm 2.6$ cm$^2$ for SEMAC-VAT and $29.8 \pm 14.7$ cm$^2$ for standard TSE, $P < 0.001$, Figure 3A). On sagittal images, the length of spinal canal obscuration around the instrumentation was significantly reduced when using SEMAC-VAT for T2-weighted imaging ($1.2 \pm 0.6$ cm vs $5.2 \pm 2.0$ cm, $P < 0.001$, Figure 3B) and T1-weighted imaging ($1.1 \pm 0.5$ cm vs $4.8 \pm 2.1$ cm, $P < 0.001$, Figure 3C).

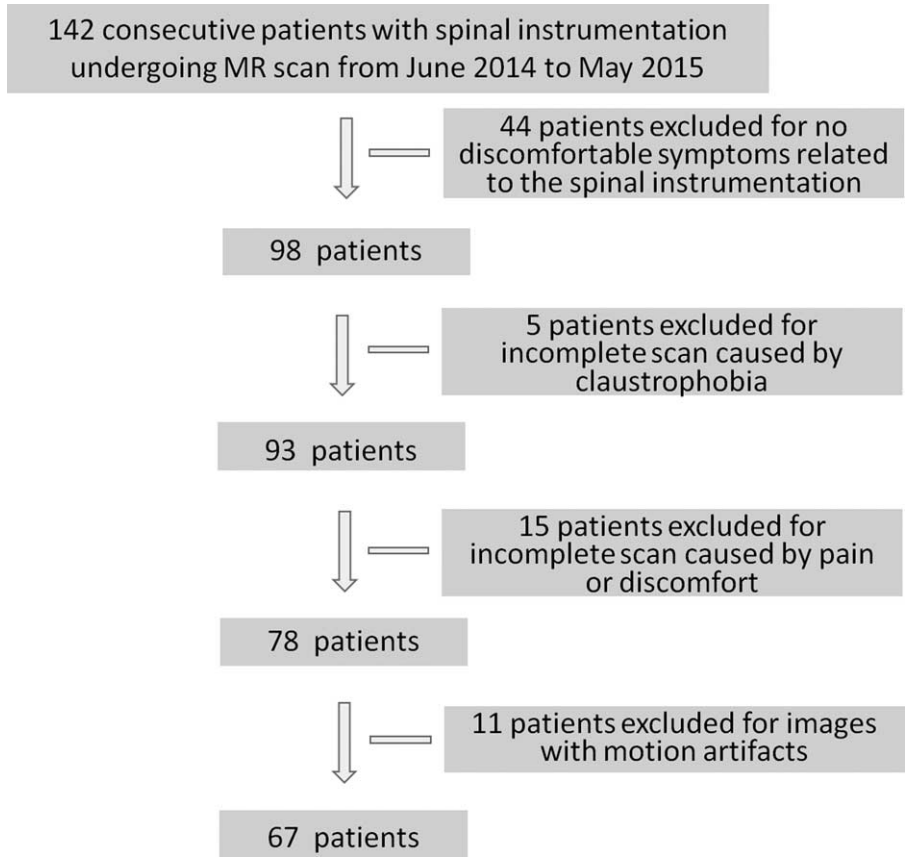


**FIGURE 2.** Patients acquirement chart.

As shown in Table 2, visualizations of all periprosthetic anatomic structures were significantly better for SEMAC-VAT TSE images compared with standard TSE images ($P < 0.001$ for all structures). Interobserver agreement for visualizations of anatomic structures was good for both SEMAC-VAT TSE (k = 0.77) and standard TSE (k = 0.74) imaging. As shown in Table 3, image quality including distortion, blurring, and image noise was significantly better for SEMAC-VAT TSE compared with standard TSE imaging ($P < 0.001$ for all). Interobserver agreement for image quality was good for SEMAC-VAT TSE (k = 0.68) and standard TSE imaging (k = 0.80).

## Clinical Results

The number of abnormal findings noted on SEMAC-VAT TSE images (59 findings) was significantly more than the number of findings detected on standard TSE images (40 findings, $P < 0.001$), with 19 (19/59 = 32.20%) of the findings missed on standard TSE images (Figure 4). All abnormal

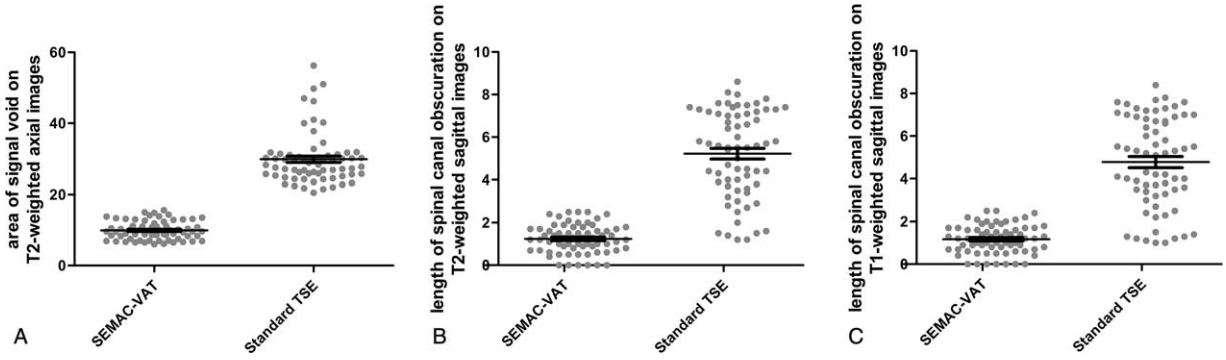


**FIGURE 3.** Spot graphs show statistic analysis results that the signal void was significantly lower in SEMAC-VAT than in standard TSE images for T2-weighted imaging (A, $P < 0.001$), and the length of spinal canal obscuration was also significantly reduced in T2-weighted imaging (B, $P < 0.001$) and T1-weighted imaging (C, $P < 0.001$). SEMAC-VAT = slice-encoding metal artifact correction–view-angle tilting, TSE = Turbo Spin Echo.

**TABLE 2.** Visualizations of Anatomic Structures

| | Reader 1 | | | Reader 2 | | | Reader 3 | | |
|---|---|---|---|---|---|---|---|---|---|
| | SEMAC-VAT | Standard TSE | *P* | SEMAC-VAT | Standard TSE | *P* | SEMAC-VAT | Standard TSE | *P* |
| Pedicle | 4.6 ± 0.9 | 2.6 ± 0.9 | <0.001 | 4.4 ± 0.8 | 2.7 ± 0.9 | <0.001 | 4.3 ± 0.5 | 2.7 ± 0.5 | <0.001 |
| Vertebral body | 4.5 ± 1.0 | 2.9 ± 1.1 | <0.001 | 4.6 ± 1.0 | 2.8 ± 1.0 | <0.001 | 4.5 ± 1.2 | 2.6 ± 0.9 | <0.001 |
| Dural sac | 3.9 ± 1.1 | 1.7 ± 0.9 | <0.001 | 3.8 ± 1.0 | 1.8 ± 0.7 | <0.001 | 3.6 ± 0.8 | 1.7 ± 0.3 | <0.001 |
| Neural | 3.7 ± 0.8 | 1.9 ± 1.0 | <0.001 | 3.6 ± 0.9 | 2.0 ± 1.0 | <0.001 | 3.4 ± 1.1 | 2.0 ± 0.6 | <0.001 |

Anatomic structures were assessed by 3 readers on a 5-point scale from 1 (not visible) to 5 (good depiction). Data are mean ± standard deviation. After Bonferroni correction, $P < 0.0125$ denotes statistical significance.

SEMAC-VAT = slice-encoding metal artifact correction–view-angle tilting, TSE = Turbo Spin Echo.

imaging findings detected on standard TSE images were also noted on SEMAC-VAT images (Figure 5). Detailed clinical findings of the subjects are displayed in Table 4. The clinical findings of spinal instrumentation adverse reaction revealed by MRI included edema, implant loosening, and fluid adjacent to metal implants. The incidence rate of spinal instrumentation adverse reaction was 38.81% ([7 of edema + 4 of implant loosening + 15 of fluid adjacent to metal implants]/67) via MRI SEMAC-VAT technique.

## DISCUSSION AND CONCLUSIONS

In this study, we systematically evaluated the diagnostic value of a SEMAC-VAT sequence in patients with spinal instrumentation. We found that the area of signal void around the instrumentation on axial images and the length of spinal canal obscuration on sagittal images significantly reduced when using SEMAC-VAT sequences. Therefore, the metal artifacts surround the implants were mostly suppressed in SEMAC-VAT images. At the same time, the number of abnormal findings on SEMAC-VAT TSE images was significantly higher than that of findings on standard TSE images, which increased the detection rate for postoperative complications around the metallic implants.

Titanium alloy hardware is more compatible with MR and has less artifacts than stainless steel and nickel.[19] However, the susceptibility artifacts around the metal, that is, the signal loss, signal pile-up, and geometric distortions, still significantly corrupt the image quality. Several practical solutions are useful for reducing the metallic artifacts, which include using fast spin echo sequences other than standard spin echo and gradient echo sequences, increasing the readout bandwidth, using inversion recovery for fat suppression rather than spectral fat saturation, reducing slice thickness and increasing image matrix.[20,21] However, none of these methods can remove metallic artifacts effectively enough for clinical diagnosis of periprostheic complications. Several more sophisticated approaches have been published. One of the first approaches is VAT, which has been available since 1988.[7] Several studies then were done to improve its performance in reducing the in-plane metallic artifacts and VAT-associated blurring.[6,8] Through-plane metallic artifacts remained a problem until the SEMAC and multi-acquisition variable-resonance image combination had been developed.[9,22] Our results showed that SEMAC and VAT effectively reduced the area of signal void and length of spinal canal obscuration around the instrumentation, which is consistent with previous studies in vivo and in vitro.[13,17,23,24] Also, the visualizations of all periprosthetic anatomic structures were significantly better for SEMAC-VAT TSE images compared with standard TSE images with a significantly improved periprosthetic visualization of the pedicle, vertebral body, dural sac, and neural foramina.

Interbody fusion with titanium screws is a widely performed surgical treatment for spinal disorders and shows good clinical results. However, patients with low-back pain and tumor recurrence are frequently seen. The SEMAC-VAT sequence provides the advantage to evaluate postoperative complications in patients, including bone marrow and soft-tissue edema, infections, tumor recurrence, and fluid adjacent to metal implants. Our results showed a general increase of diagnostic accuracy for all these complications when using SEMAC-VAT. Furthermore, in some cases, where the complications were also visible in the standard TSE images, SEMAC-

**TABLE 3.** Effect of Metal Artifacts on Image Quality

| | Reader 1 | | | Reader 2 | | | Reader 3 | | |
|---|---|---|---|---|---|---|---|---|---|
| | SEMAC-VAT | Standard TSE | *P* | SEMAC-VAT | Standard TSE | *P* | SEMAC-VAT | Standard TSE | *P* |
| Distortion | 4.8 ± 0.8 | 2.2 ± 0.5 | <0.001 | 4.6 ± 0.7 | 2.1 ± 0.3 | < 0.001 | 4.7 ± 0.8 | 2.4 ± 0.9 | <0.001 |
| Blurring | 4.4 ± 0.7 | 2.4 ± 0.3 | <0.001 | 4.5 ± 0.4 | 2.5 ± 0.6 | < 0.001 | 4.6 ± 0.3 | 2.3 ± 0.6 | <0.001 |
| Noise | 3.9 ± 0.6 | 2.1 ± 0.3 | <0.001 | 3.7 ± 0.5 | 2.3 ± 0.4 | < 0.001 | 3.8 ± 0.6 | 2.3 ± 0.5 | <0.001 |

Distortion, blurring, and image noise were assessed by 3 readers on a 5-point scale from 1 (severe artifacts and nondiagnostic image) to 5 (no artifacts). Data are mean ± standard deviation. After Bonferroni correction, $P < 0.0167$ denotes statistical significance.

SEMAC-VAT = slice-encoding metal artifact correction–view-angle tilting, TSE = Turbo Spin Echo.

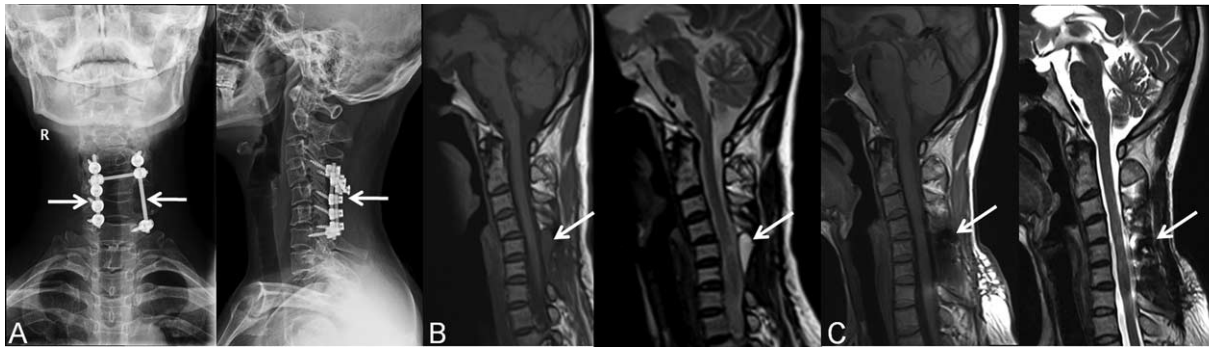


**FIGURE 4.** A 42-year-old female who had cervical spinal schwannomaon C5–6 level and performed surgical resection. The follow-up posterioranterior and lateral x-ray films (A, arrows) show the cervical instrumentation. The follow-up sagittal T1 and T2 images with SEMAC-VAT show fluid accumulation (B, arrows) behind the C5–6 vertebral body and spinal cords welling. However, sagittal T1 and T2 images with standard TSE missed the fluid (C, arrows). SEMAC-VAT = slice-encoding metal artifact correction–view-angle tilting, TSE = Turbo Spin Echo.

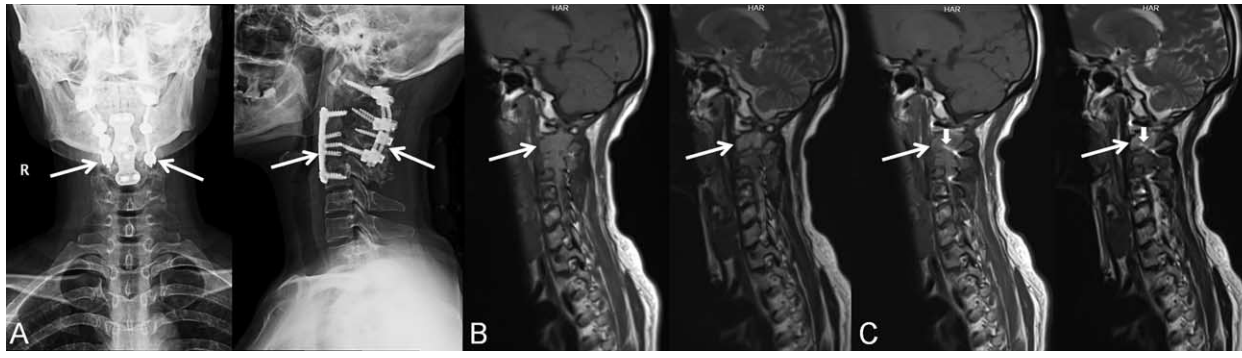


**FIGURE 5.** A 37-year-old female with the recurrence of giant cell tumor of the cervical spine on C2–3 level after surgical resection. The follow-up posterioranterior and lateral x-ray films (A, arrows) show the cervical instrumentation. The follow-up sagittal T1 and T2 images with SEMAC-VAT (B) and standard TSE (C) show a mass in C2 and C3 vertebral bodies and the mass extends into the spinal canal and pushes back the spinal canal (B and C, long arrows). However, images with standard TSE have obvious metal artifacts (C, short arrows). SEMAC-VAT = slice-encoding metal artifact correction–view-angle tilting, TSE = Turbo Spin Echo.

VAT provided a better image quality for reducing the susceptibility artifacts.

The incidence rate of spinal instrumentation adverse reaction was 38.81% via MRI SEMAC-VAT technique in this study. The clinical findings of spinal instrumentation adverse reaction revealed by MRI included edema, implant loosening, and fluid adjacent to metal implants. Patients with discomfort hallmarks excluding recurrent neoplasm, recurrent disc herniation, and infection factors, are adverse reaction population. Presurgery informed consent and better communications with patients might improve mutual understanding between doctors and patients. Suspected patients with discomfort should undergo MRI with SEMAC-VAT sequence. More profound studies are needed to eliminate or alleviate the adverse reaction.

**TABLE 4.** Detailed Clinical Findings of the Subjects

| Findings | SEMAC-VAT | Standard TSE |
|---|---|---|
| Edema | 7 | 5 |
| Tumor recurrence | 9 | 6 |
| Infection | 8 | 5 |
| Implant loosening | 4 | 2 |
| Disc herniation recurrence | 16 | 12 |
| Fluid adjacent to metal implants | 15 | 10 |
| Total | 59 | 40 |

SEMAC-VAT = slice-encoding metal artifact correction–view-angle tilting, TSE = Turbo Spin Echo.

One limitation in our study is that the z-phase encoding range applied for SEMAC was not sufficient for optimal distortion correction.[9,10] Our preliminary test showed that the optimal number for z-phase-encoding steps is 15, while larger values do not improve the image quality anymore. However, the trade off is that scan time was prolonged to about 15 minutes. Thus, to improve the acceptance in clinical imaging, we reduced the z-phase-encoding steps to 6, which suppressed most of the metal artifacts in <3 minutes in T2 imaging and 5 minutes in T1 imaging. The other limitation is that short tau inversion recovery images with SEMAC-VAT were not included in this study. STIR images can provide higher tissue contrast by suppressing fat signal, and are useful for detecting small fluid signals in spinal diseases. However, scan time of this sequence with SEMAC-VAT is too long for clinical use, and is hard for

patients to tolerate the total MR scan. Further MR techniques to reduce the scan time will benefit its clinical practice.

In conclusion, MR images with SEMAC-VAT can significantly reduce metal artifacts for spinal instrumentation and improve delineation of the instrumentation and periprosthetic region. SEMAC-VAT technique can improve image quality and diagnostic accuracy in patients with postinstrumentation spinal diseases. Suspected patients with discomfort undergoing MRI with SEMAC-VAT sequence may reveal pathologic mechanisms.

## ACKNOWLEDGMENTS

*The authors would like to thank the subjects participating in this study and Ling Wang (Department of Health Statistics, Faculty of Preventive Medicine, the Fourth Military Medical University, Xi'an, PR China) for the statistical analysis of this study.*

## REFERENCES

1. Ludeke KM, Roschmann P, Tischler R. Susceptibility artefacts in NMR imaging. *Magn Reson Imaging.* 1985;3:143–329.
2. Viano AM, Gronemeyer SA, Haliloglu M, et al. Improved MR imaging for patients with metallic implants. *Magn Reson Imaging.* 2000;18:287–295.
3. Camacho CR, Plewes DB, Henkelman RM. Nonsusceptibility artifacts due to metallic objects in MR imaging. *J Magn Reson Imaging.* 1995;5:75–88.
4. Hargreaves BA, Worters PW, Pauly KB, et al. Metal-induced artifacts in MRI. *AJR Am J Roentgenol.* 2011;197:547–555.
5. Gupta A, Subhas N, Primak AN, et al. Metal artifact reduction: standard and advanced magnetic resonance and computed tomography techniques. *Radiol Clin North Am.* 2015;53:531–547.
6. Butts K, Pauly JM, Gold GE. Reduction of blurring in view angle tilting MRI. *Magn Reson Med.* 2005;53:418–424.
7. Cho ZH, Kim DJ, Kim YK. Total inhomogeneity correction including chemical shifts and susceptibility by view angle tilting. *Med Phys.* 1988;15:7–11.
8. Kolind SH, MacKay AL, Munk PL, et al. Quantitative evaluation of metal artifact reduction techniques. *J Magn Reson Imaging.* 2004;20:487–495.
9. Lu W, Pauly KB, Gold GE, et al. SEMAC: slice encoding for metal artifact correction in MRI. *Magn Reson Med.* 2009;62:66–76.
10. Lu W, Pauly KB, Gold GE, et al. Slice encoding for metal artifact correction with noise reduction. *Magn Reson Med.* 2011;65:1352–1357.
11. Friedrich B, Wostrack M, Ringel F, et al. Novel metal artifact reduction techniques with use of slice-encoding metal artifact correction and view-angle tilting MR imaging for improved visualization of brain tissue near intracranial aneurysm clips. *Clin Neuroradiol.* 2014[Epub ahead of print].
12. Lee YH, Lim D, Kim E, et al. Feasibility of fat-saturated T2-weighted magnetic resonance imaging with slice encoding for metal artifact correction (SEMAC) at 3T. *Magn Reson Imaging.* 2014;32:1001–1005.
13. Ai T, Padua A, Goerner F, et al. SEMAC-VAT and MSVAT-SPACE sequence strategies for metal artifact reduction in 1.5T magnetic resonance imaging. *Invest Radiol.* 2012;47:267–276.
14. Song KD, Yoon YC, Park J. Reducing metallic artefacts in postoperative spinal imaging: slice encoding for metal artefact correction with dual-source parallel radiofrequency excitation MRI at 3.0 T. *Br J Radiol.* 2013;86:20120524.
15. Griffin JFt, Archambault NS, Mankin JM, et al. Magnetic resonance imaging in cadaver dogs with metallic vertebral implants at 3 Tesla: evaluation of the WARP-turbo spin echo sequence. *Spine (PhilaPa 1976).* 2013;38:E1548–E1553.
16. Chen CA, Chen W, Goodman SB, et al. New MR imaging methods for metallic implants in the knee: artifact correction and clinical impact. *J Magn Reson Imaging.* 2011;33:1121–1127.
17. Lee YH, Lim D, Kim E, et al. Usefulness of slice encoding for metal artifact correction (SEMAC) for reducing metallic artifacts in 3-T MRI. *Magn Reson Imaging.* 2013;31:703–706.
18. Sutter R, Ulbrich EJ, Jellus V, et al. Reduction of metal artifacts in patients with total hip arthroplasty with slice-encoding metal artifact correction and view-angle tilting MR imaging. *Radiology.* 2012;265:204–214.
19. Ahmad FU, Sidani C, Fourzali R, et al. Postoperative magnetic resonance imaging artifact with cobalt-chromium versus titanium spinal instrumentation: presented at the 2013 Joint Spine Section Meeting. Clinical article. *J Neurosurg Spine.* 2013;19:629–636.
20. Lee MJ, Kim S, Lee SA, et al. Overcoming artifacts from metallic orthopedic implants at high-field-strength MR imaging and multidetector CT. *Radiographics.* 2007;27:791–803.
21. Vandevenne JE, Vanhoenacker FM, Parizel PM, et al. Reduction of metal artefacts in musculoskeletal MR imaging. *JBR-BTR.* 2007;90:345–349.
22. Koch KM, Lorbiecki JE, Hinks RS, et al. A multispectral three-dimensional acquisition technique for imaging near metal implants. *Magn Reson Med.* 2009;61:381–390.
23. Månsson S, Müller GM, Wellman F, et al. Phantom based qualitative and quantitative evaluation of artifacts in MR images of metallic hip prostheses. *Phys Med.* 2015;31:173–178.
24. Müller GM, Lundin B, von Schewelov T, et al. Evaluation of metal artifacts in clinical MR images of patients with total hip arthroplasty using different metal artifact-reducing sequences. *Skeletal Radiol.* 2015;44:353–359.